Low Loss Ultra-Small Core Pitch All-Fiber Fan-In/Fan-Out Device For Coupled-Core Multicore Fibers

Junjie Xiong, Lin Ma, *Member, IEEE*, Ying Shi, Linbin Bai, and Zuyuan He, *Senior Member, IEEE*

***Abstract*—We designed and fabricated all-fiber fan-in/fan-out (FI/FO) devices using a fused taper technique for square lattice structure coupled-core multicore fiber (CC-MCF). A vanishing core bridge fiber with a diameter of 80 μm was tailor-designed to minimize both the mode field mismatch and the required tapering ratio at the same time. In experiment, we succeeded in fabricating FI/FO devices with a core pitch as small as 17 μm and achieving practically low insertion losses of 1.43 dB and 2.28 dB for fan-in and fan-out devices, respectively. The fabricated FI/FO devices can well multiplex and demultiplex 1550 nm light into and out from the CC-MCF without obvious total power fluctuation even when an external perturbation is intentionally imposed on the CC-MCF. The proposed FI/FO device is very useful for both the study and application of CC-MCFs which usually have ultra-small core pitches.**

***Index Terms*—Coupled-core multicore fiber, fan-in and fan-out device, space division multiplexing.**

I. Introduction

IN ORDER to satisfy the dramatically increasing demands for data transmission capacity, multicore fibers (MCFs) are considered to be promising transmission media. They have been intensively investigated to keep the system within a manageable power consumption and cost budget [1], [2], [3], [4], [5]. As vital interface devices to couple light between MCFs and traditional single-core fibers (SCFs), the fan-in/fan-out (FI/FO) devices are indispensable for applications using MCFs. Recently, coupled-core multicore fibers (CC-MCFs) have drawn a lot of attention due to their distinctive advantages such as reduced group delay spread [6] and mitigation of fiber nonlinearities [7] which make them particularly attractive for long-haul transmission applications [8], [9], [10], [11]. However, CC-MCFs usually require a core pitch design smaller than 30 μm to realize the desirable inter-core mode coupling, which is challenging for the design and fabrication of compatible FI/FO devices.

Manuscript received 19 July 2022; revised 5 August 2022; accepted 8 August 2022. Date of publication 11 August 2022; date of current version 22 August 2022. The work was supported in part by the National Key R&D Program of China under Grant 2018YFB1801000 and in part by the National Natural Science Foundation of China under Grant 61835006. *(Corresponding author: Lin Ma.)*

Junjie Xiong, Lin Ma, Ying Shi, and Zuyuan He are with the State Key Laboratory of Advanced Optical Communication Systems and Networks, Shanghai Jiao Tong University, Shanghai 200240, China (e-mail: xiongjunjie@sjtu.edu.cn; ma.lin@sjtu.edu.cn; yingshi@sjtu.edu.cn; zuyuanhe@sjtu.edu.cn).

Linbin Bai is with the Shanghai Optoweave Technology Co., Ltd., Shanghai 200240, China (e-mail: bai.linbin@optoweave.com).

Digital Object Identifier 10.1109/JPHOT.2022.3198087

Several FI/FO devices have been demonstrated based on all-fiber [12], [13], [14], [15], [16], [17], [18], femtosecond laser inscription [19], [20], and lens optics [21], [22] method. The FI/FO devices fabricated by the femtosecond laser inscription technique can achieve high alignment accuracy and integration density. However, it is difficult to reduce their insertion losses due to the mode field mismatch and the nature of point-by-point fabrication. The lens type FI/FO devices can achieve low loss, while they require precise alignment and expensive free-space optics systems.

All-fiber type FI/FO devices have advantages such as low loss, low polarization-dependent loss, and high compatibility with MCFs and SCFs. Typical all-fiber type FI/FO devices include fiber bundle [12], [13] and fused taper types [14], [15], [16], [17], [18]. The fiber bundle type FI/FO devices are usually fabricated by inserting a bundle of etched fibers into the ceramic ferrule. This process is challenging for MCF with a core pitch less than 30 μm because the etched fiber is very fragile. Some fused taper type FI/FO devices designed for CC-MCF with a small core pitch of 20-30 μm were demonstrated with commercially available few-mode fiber [8], [9] or graded-index multi-mode fiber [18] as bridge fibers for tapering. However, these bridge fibers were difficult to simultaneously achieve low coupling loss with SCFs and MCFs due to the mode field mismatch.

On the other hand, using vanishing core fiber (VCF) as bridge fibers for fused taper type FI/FO devices, which was first proposed in [15], has been proved to be an effective way to realize low-loss connection between SCFs and MCF. The VCF design usually consists of three refractive index layers. Before tapering process, the inner two layers are used to minimize the mode field mismatch with the SCFs. After tapering process, the overall structure shrinks in size. The inner two layers constitute the new core and the outmost layer becomes the new cladding. The tapered VCF is used to realize mode field matching with MCFs. Several types of VCF designs [15], [16], [17] have been reported in FI/FO devices for weakly coupled multicore fibers with core pitches larger than 35 μm.

In this work, we demonstrate all-fiber FI/FO devices for a square lattice structure coupled-core four-core fiber (CC-4CF) with the smallest core pitch (17 μm), of its kind to the best of our knowledge. A new vanishing core bridge fiber (VCBF) was tailor designed with a thin cladding of 80 μm to minimize the mode field mismatch for this fused taper type FI/FO device. In experiment, the fabricated fan-in and fan-out devices achieved

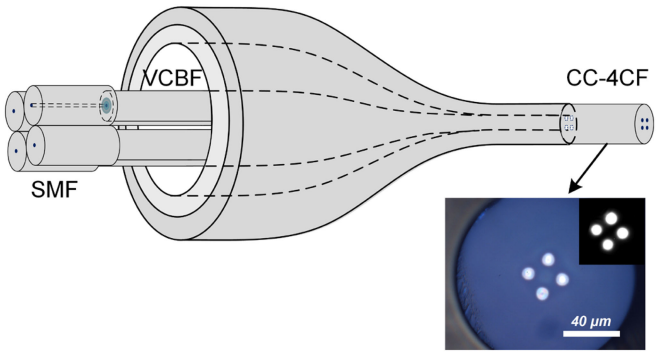

Fig. 1. The schematic of all-fiber FI/FO device using a fused taper technique and cross-sectional micrograph of the fabricated CC-4CF.

practically low average insertion losses of 1.43 dB and 2.28 dB, respectively. They show acceptable channel uniformity and can multiplex and demultiplex 1550 nm light into and out from the CC-MCF without obvious total power fluctuation even under the condition of strong random energy exchange among the cores by intentionally imposing an external perturbation on the CC-MCF. The demonstrated FI/FO devices pave the way for the applications of CC-MCFs and are very useful for studying their strong mode coupling effect.

II. Principle and Design

The proposed all-fiber FI/FO device for interfacing SSMFs and a CC-4CF is shown in Fig. 1. It consists of a glass capillary and bridge fibers with a vanishing core design. The close-packed VCBFs are inserted in the capillary and tapered down to match the structure of CC-4CF. The taper ratio of the FI/FO device is calculated from the ratio of the VCBF diameter to the core pitch of the CC-4CF. Four SSMFs are spliced to VCBFs on the left and the end-face of the device consisting of a tapered VCBF bundle is spliced to a CC-4CF on the right, respectively. The FI/FO device is designed for a fabricated CC-4CF with a square lattice structure whose cross-sectional image is shown in Fig. 1. The core pitch and cladding diameter of the CC-4CF are 17 μm and 125 μm, respectively. The CC-4CF used in this paper was designed and fabricated by ourselves. Individual core design of the CC-4CF is in accordance with ITU-T recommendation G.652D. The optimum core pitch of 17 μm is used to realize low spatial mode dispersion of the designed CC-4CF.

In order to minimize the coupling loss of the FI/FO device with both the SSMF and CC-4CF, a VCF approach was used to realize mode field matching. Fig. 2 shows the designed VCBF with a four-layer step-index design. The trench structure with an index of n_3 is added to reduce the bending loss and prevent mode field leakage to outer cladding. Moreover, improvements of 80-μm-diameter cladding have been made in our VCBF design to make it suitable for the FI/FO device with small core pitch. The small core pitch requires a large taper ratio. In general, the larger taper ratio makes the realization of the adiabatic taper condition more difficult. The designed thin cladding reduces the taper ratio to about 4.7, which decreases by 1.56 times compared with the

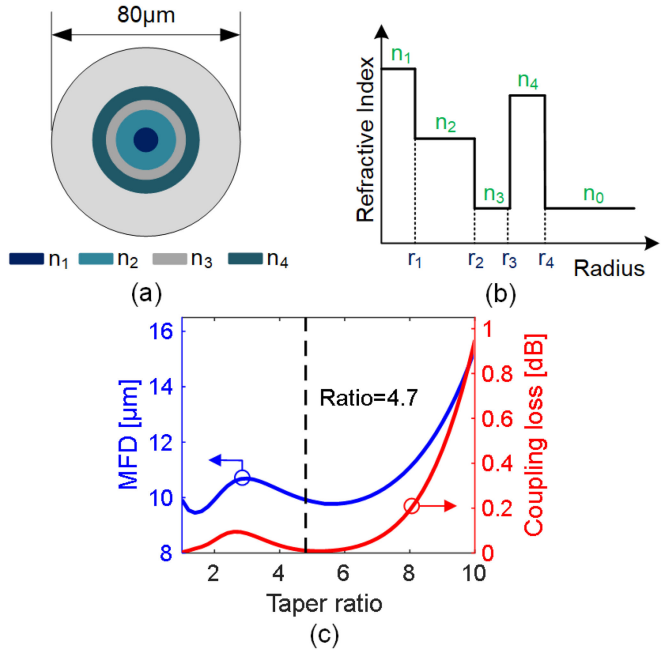

Fig. 2. (a) Cross section and (b) index profile of designed VCBF; (c) simulated MFD and coupling loss with SSMF of designed VCBF as functions of tapering ratios.

TABLE I
Designed Parameters of the VCBF

Radius (μm)	r_1	r_2	r_3	r_4	$r_{cladding}$
	4.1	12.1	16.1	20.6	40
Refractive index (RIU)	n_1	n_2	n_3	n_4	n_0
	1.4545	1.4494	1.4440	1.4525	1.4440

usual 125-μm cladding. Overall, the improved design facilitates the fabrication process. The parameters of each layer were tailor designed to make the designed VCBF suitable for the FI/FO with small core pitch of 17 μm. The parameters of the designed VCBF are listed in Table I.

Fig. 2(c) shows the mode field diameter (MFD) of the designed VCBF at different taper ratios calculated by a finite element method. The coupling loss between the VCBF and the SSMF as a function of taper ratios was calculated by integral overlap of the mode fields. As shown by the red line in Fig. 2(c), theoretical coupling losses smaller than 0.1 dB at both sides of the FI/FO device can be achieved when the taper ratios of the VCBF are 1 and 4.7 (same for the FI/FO device), at which MFDs of the VCBF at 1550 nm before and after tapering are 9.9 μm and 10.1 μm, respectively.

III. Fabrication

The VCBF was fabricated by a state-of-the-art plasma chemical vapor deposition (PCVD) method. Its cross-sectional micrograph and measured index profile are shown in Fig. 3. The measured MFD of the VCBF is 9.1 μm at 1550 nm, and both the measured index profile and MFD agree well with the

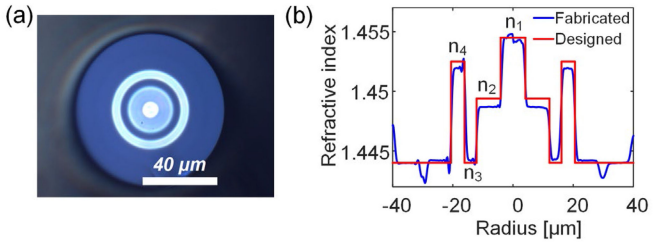

Fig. 3. (a) Cross-sectional micrograph and (b) index profile of the fabricated VCBF.

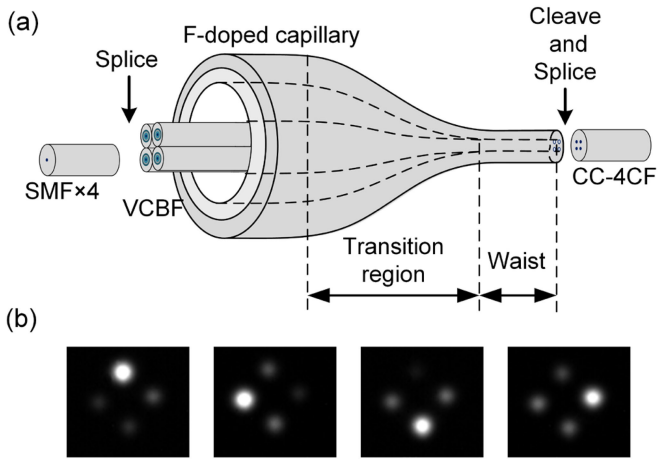

Fig. 4. (a) Schematic view of device fabrication; (b) Measured intensity profile at the taper end face for different input ports.

designed ones. The attenuation of the VCBF was measured to be 0.24 dB/km at 1550 nm using an optical time-domain reflectometer (OTDR). The splicing loss between the fabricated VCBF and the SSMF was measured to be 0.11 dB.

Fig. 4(a) shows the fabrication schematic of the FI/FO device. First, four VCBFs were inserted into a fluorine-doped (F-doped) capillary and co-tapered to a ratio of about 4.7 using a Fujikura LZM-100 CO_2 laser processing station. In order to achieve adiabatic tapering condition and reduce the excess loss, the length of the taper transition region is set to be longer than 10 mm. Second, the tapered bundle was cleaved at the waist region using a high-precision fiber cleaver (Fujikura CT106), and the cross-sectional image of the taper end face is shown in Fig. 5(a). A perfect square lattice arrangement was successfully maintained even after tapering process with a ratio as large as 4.7 and the measured core pitch was about 17 μm with a deviation less than 0.5 μm. The near field profiles at the tapered end of the device with light input from different ports are shown in Fig. 4(b). It can be observed that the tapered bundle operates well at a wavelength of 1550 nm. To characterize its insertion loss of the individual channels, a large-area free-space photodetector was used to collect the optical power at the end face of tapered bundles. As shown in Table II, measured average insertion losses at 1550 nm are 0.21 dB and 0.23 dB for the fan-in and fan-out devices, respectively.

The tapered bundle was then spliced to a piece of 5-meter-long CC-4CF using a Fujikura FSM-100P+ splice machine to

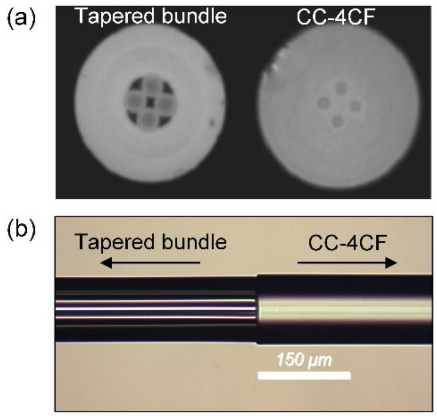

Fig. 5. (a) Cross-sectional image of the end face of the tapered bundle and CC-4CF, respectively; (b) microscopic image of the splice point.

TABLE II
INSERTION LOSS OF THE TAPERED BUNDLES

	Port 1	Port 2	Port 3	Port 4	Avg.
Tapered bundle of fan-in device (dB)	0.21	0.33	0.17	0.12	0.21
Tapered bundle of fan-out device (dB)	0.32	0.15	0.24	0.19	0.23

TABLE III
INSERTION LOSS OF THE FABRICATED FI/FO DEVICES

	Port 1	Port 2	Port 3	Port 4	Avg.
Fan-in device (dB)	1.89	1.42	1.03	1.39	1.43
Fan-out device (dB)	2.66	2.32	2.89	1.24	2.28

function as FI/FO devices. As shown in Fig. 5(b), a uniform interface between the tapered bundle and the CC-4CF was achieved, indicating no deformation during the splicing. The insertion loss of the FI/FO devices was measured and the result is shown in Table III. A large-area free-space photodetector was adopted to receive optical power from all cores of the CC-4CF. The average insertion losses are 1.43 dB and 2.28 dB at 1550 nm for the fan-in and fan-out devices, respectively. The insertion losses of the fabricated fan-in and fan-out devices are mainly induced by the fiber deformation during the tapering process and the misalignment during the splicing process. These can be mitigated by further optimizing the fabrication process.

IV. CHARACTERISTICS OF FI/FO DEVICES

The characteristics of a pair of FI/FO devices were investigated using an experimental setup as shown in Fig. 6. The fan-in and fan-out devices were spliced to the two ends of a piece of 5-m-long CC-4CF, respectively. We used an external-cavity laser (Osics T100) operating at a wavelength of 1550 nm as the light source. The light was coupled into the CC-4CF through the fan-in device and a 4-channel power meter (Santec MPM-200) was used to simultaneously receive the optical power of the four output ports of the fan-out device. Due to the intrinsic inter-core

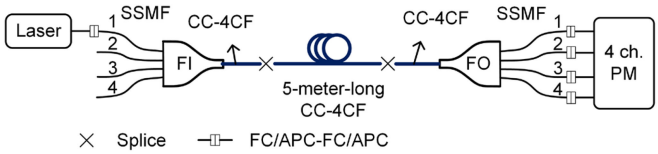

Fig. 6. Experimental setup for optical characteristics measurement of a pair of FI/FO devices.

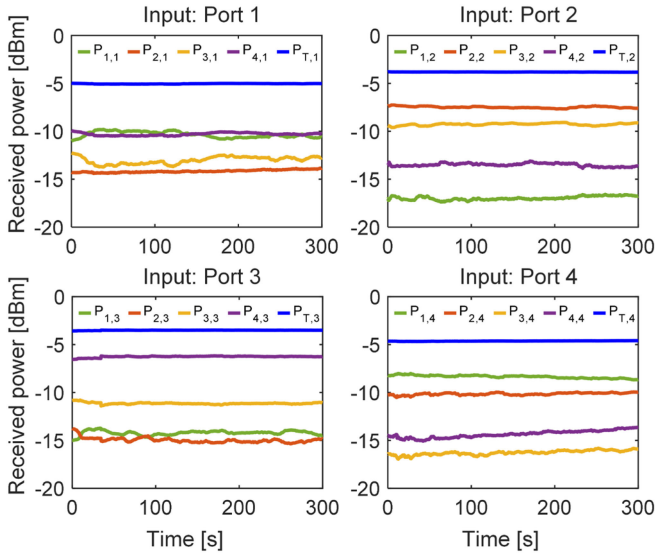

Fig. 7. The received power of a pair of FI/FO devices with 5-m CC-4CF for different input ports during 300 seconds. The input power is 1 mW.

mode coupling, the power in the cores of CC-4CF will exchange among all cores.

The insertion losses of the FI/FO devices are defined as

$$IL_{i,j} = -10 \cdot \lg\left(\frac{P_{i,j}}{P_{in}}\right) \quad (1)$$

$$IL_{T,j} = -10 \cdot \lg\left(\frac{\sum_{i=1}^{4} P_{i,j}}{P_{in}}\right) = -10 \cdot \lg\left(\frac{P_{T,j}}{P_{in}}\right) \quad (2)$$

where $P_{i,j}$ and $IL_{i,j}$ represent the received optical power and insertion loss, and the subscripts represent the output port $i(i = 1, 2, 3, 4)$ and input port $j(j = 1, 2, 3, 4)$, respectively. P_{in} is the input power, which is set to be 1 mW in our experiments. The total received power $P_{T,j}$ is defined as the sum of four outputs for each input port, and the total insertion loss $IL_{T,j}$ is calculated from (2).

Fig. 7 shows the measured output power at the fan-out ports when light is input from different ports in an observation time of 300 seconds. Although the light is mainly coupled into one of the cores of the CC-4CF at the fan-in side, it will be randomly coupled to the other cores due to the intrinsic inter-core mode coupling and fluctuations in the received power of individual cores can be observed. On the other hand, $P_{T,j}$ remains stable over time with a standard deviation of less than 0.022 dB. The total insertion losses for different input ports are shown in Table IV. The maximum $IL_{T,j}$ achieved is about 5.0 dB, which is practically low for both characterization and transmission

TABLE IV
THE TOTAL INSERTION LOSS OF THE FI/FO PAIRS

	Port 1	Port 2	Port 3	Port 4
Avg. (dB)	5.03	3.81	3.50	4.63
Std. (dB)	0.022	0.009	0.017	0.022

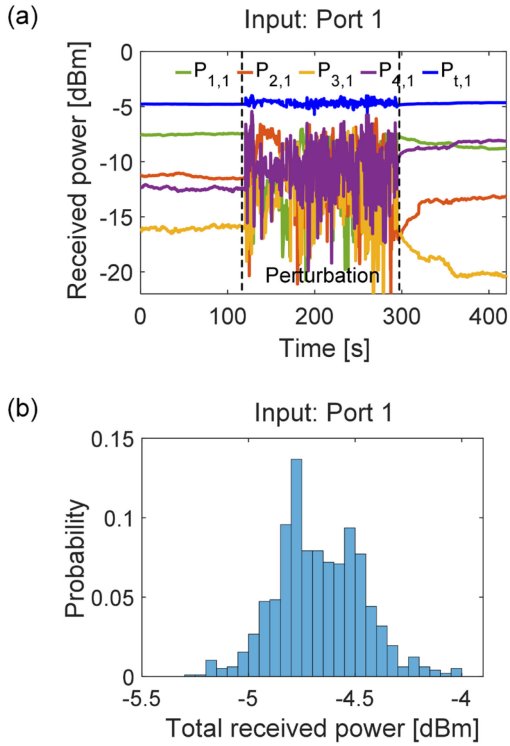

Fig. 8. (a) The received optical power with fiber perturbation when light is coupled into input port 1; (b) the probability distribution of the total received optical power.

purposes. The wavelength dependence of the FI/FO link was investigated. The total insertion loss and the fluctuation of each port are lower than 5.2 dB and 1 dB over the C-band.

The characteristic of the FI/FO devices with perturbation was experimentally investigated and the results are shown in Fig. 8. Random perturbation was intentionally applied to the CC-4CF by continuously scratching the fiber. This perturbation includes not only vibration, but also the continuous deformation of the fiber such as twisting and bending. It can be observed that although there is a dramatic power coupling among all cores, the optical power in each core of the CC-4CF can still be well demultiplexed by the fan-out device with almost constant total received power. As shown in Fig. 8(b), the average total insertion loss during the perturbation is 4.71 dB with a standard deviation of about 0.151 dB, which probably resulted from the differences in insertion loss among individual ports of the FI/FO devices and can be minimized by further improving the fabrication process. After the external perturbation was stopped, the relative power in each port did not return to its initial level because the inter-core coupling state of the CC-4CF was changed due to the external disturbance such as changes in twisting and bending conditions.

However, the total power of the 4 cores remains almost the same after the perturbation and the level of fluctuation in the power of each core would gradually return to its original value when the fiber was stable. In the case of real application, the coupling status of the CC-4CF will not change dramatically in a short time, and the gradual changes in coupling status which may result in changes in received power of individual core can be equalized by implementation of the digital signal process (DSP) technique.

V. Conclusion

We designed and fabricated all-fiber FI/FO devices for a square lattice structure CC-4CF with a core pitch as small as 17 μm, which shows practically low average insertion loss of 1.43 dB and 2.28 dB for fan-in and fan-out devices, respectively. It was experimentally demonstrated that the light can be well multiplexed and demultiplexed into and out from the CC-4CF with a small total power fluctuation even under strong random energy exchange among cores when external perturbation was imposed on the CC-4CF. As a result, the proposed FI/FO device is very useful for both the study and application of CC-MCFs with an ultra-small core pitch design.

References

[1] K. Saitoh and S. Matsuo, "Multicore fiber technology," *J. Lightw. Technol.*, vol. 34, no. 1, pp. 55–66, Jan. 2016.

[2] B. J. Puttnam, G. Rademacher, and R. S. Luís, "Space-division multiplexing for optical fiber communications," *Optica*, vol. 8, no. 9, pp. 1186–1203, 2021.

[3] T. Sakamoto et al., "Six-mode seven-core fiber for repeated dense space-division multiplexing transmission," *J. Lightw. Technol.*, vol. 36, no. 5, pp. 1226–1232, Mar. 2018.

[4] Y. Liu, L. Ma, C. Yang, W. Tong, and Z. He, "Multimode and single-mode fiber compatible graded-index multicore fiber for high density optical interconnect application," *Opt. Exp.*, vol. 26, no. 9, pp. 11639–11648, 2018.

[5] T. Hayashi et al., "125-μm-cladding eight-core multi-core fiber realizing ultra-high-density cable suitable for O-Band short-reach optical interconnects," *J. Lightw. Technol.*, vol. 34, no. 1, pp. 85–92, Jan. 2016.

[6] T. Sakamoto, T. Mori, M. Wada, T. Yamamoto, F. Yamamoto, and K. Nakajima, "Fiber twisting- and bending-induced adiabatic/nonadiabatic super-mode transition in coupled multicore fiber," *J. Lightw. Technol.*, vol. 34, no. 4, pp. 1228–1237, Feb. 2016.

[7] R. Ryf, N. K. Fontaine, H. Chen, and R.-J. Essiambre, "Coupled-core fibers: Where mode scrambling mitigates nonlinear effects," in *Proc. OSA APC*, 2017, Paper NeTh2B.2.

[8] R. Ryf et al., "Long-distance transmission over coupled-core multicore fiber," in *Proc. Post Deadline Paper; 42nd Eur. Conf. Opt. Commun.*, 2016, pp. 1–3.

[9] R. Ryf et al., "Coupled-core transmission over 7-core fiber," in *Proc. Opt. Fiber Commun. Conf. Exhib.*, 2019, Paper Th4B.3.

[10] T. Hayashi, Y. Tamura, T. Hasegawa, and T. Taru, "Record-low spatial mode dispersion and ultra-low loss coupled multi-core fiber for ultra-long-haul transmission," *J. Lightw. Technol.*, vol. 35, no. 3, pp. 450–457, Feb. 2017.

[11] G. Rademacher et al., "High capacity transmission in a coupled-core three-core multi-core fiber," *J. Lightw. Technol.*, vol. 39, no. 3, pp. 757–762, Feb. 2021.

[12] K. Shikama, Y. Abe, H. Ono, and A. Aratake, "Low-loss fiber-bundle-type fan-in/fan-out device for 6-mode 19-core fiber," in *Proc. Opt. Fiber Commun. Conf. Exhib.*, 2017, pp. 1–3.

[13] K. Kawasaki, T. Sugimori, K. Watanabe, T. Saito, and R. Sugizaki, "Four-fiber fan-out for MCF with square lattice structure," in *Proc. Opt. Fiber Commun. Conf. Exhib.*, 2017, Paper W3H.4.

[14] K. Omichi et al., "Multi-core to 7 single-core-fibers fan-out device with multi-core fiber pigtail connector," in *Proc. 23rd Int. Conf. Opt. Fiber Sensors*, 2014, pp. 429–432.

[15] V. I. Kopp, J. Park, M. Wlodawski, J. Singer, D. Neugroschl, and A. Z. Genack, "Pitch reducing optical fiber array for dense optical interconnect," in *Proc. IEEE Avionics, Fiber-Opt. Photon. Dig.*, 2012, pp. 48–49.

[16] V. I. Kopp, J. Park, J. Singer, D. Neugroschl, and A. Gillooly, "Low return loss multicore fiber-fanout assembly for SDM and sensing applications," in *Proc. Opt. Fiber Commun. Conf. Exhib.*, 2020, Paper M2C.3.

[17] L. Gan et al., "Ultra-low crosstalk fused taper type fan-in/fan-out devices for multicore fibers," in *Proc. Opt. Fiber Commun. Conf. Exhib.*, 2019, pp. 1–3.

[18] S. van der Heide et al., "Low-loss low-mdl core multiplexer for 3-core coupled-core multi-core fiber," in *Proc. Opt. Fiber Commun. Conf. Exhib.*, 2020, pp. 1–3.

[19] R. R. Thomson et al., "Ultrafast-laser inscription of a three dimensional fan-out device for multicore fiber coupling applications," *Opt. Exp.*, vol. 15, no. 18, pp. 11691–11697, 2007.

[20] Y.-C. Ling, S. Yuan, and S. B. Yoo, "Low-loss three-dimensional fan-in/fan-out devices for multi-core fiber integration," in *Proc. Opt. Fiber Commun. Conf. Exhib.*, 2021, pp. 1–3.

[21] T. Takahata, A. Kaya, Y. Ozawa, Y. Minagawa, and T. Kobayashi, "High reliability fan-in/fan-out device with isolator for multi-core fibre based on free space optics," in *Proc. Eur. Conf. Opt. Commun.*, 2021, pp. 1–3.

[22] Y. Tottori, T. Kobayashi, and M. Watanabe, "Low loss optical connection module for seven-core multicore fiber and seven single-mode fibers," *IEEE Photon. Technol. Lett.*, vol. 24, no. 21, pp. 1926–1928, Nov. 2012.